Journal of Radiation Research, Vol. 58, No. 4, 2017, pp. 523–528
doi: 10.1093/jrr/rrx002
Advance Access Publication: 1 February 2017

Estimation of whole-body radiation exposure from brachytherapy for oral cancer using a Monte Carlo simulation

Y. Ozaki[1], H. Watanabe[1,*], A. Kaida[2], M. Miura[2], K. Nakagawa[3], K. Toda[3], R. Yoshimura[3], Y. Sumi[4] and T. Kurabayashi[1]

[1]Department of Oral and Maxillofacial Radiology, Graduate School, Tokyo Medical and Dental University, Yushima 1-5-45, Bunkyo-ku, Tokyo, 113-8549, Japan
[2]Department of Oral Radiation Oncology, Graduate School, Tokyo Medical and Dental University, Yushima 1-5-45, Bunkyo-ku, Tokyo, 113-8549, Japan
[3]Department of Radiation Therapeutics and Oncology, Graduate School, Tokyo Medical and Dental University, Yushima 1-5-45, Bunkyo-ku, Tokyo, 113-8549, Japan
[4]Center of Advanced Medicine for Dental and Oral Diseases, National Center for Geriatrics and Gerontology, Moriokacho 7-430, Obu-shi, Aichi, Obu, 474-8511, Japan
*Corresponding author. Department of Oral and Maxillofacial Radiology, Graduate School, Tokyo Medical and Dental University, Yushima 1-5-45, Bunkyo-ku, Tokyo, 113-8549, Japan. Tel: +81-3-5803-5545; Fax: +81-3-5803-0205; Email: hiro.orad@tmd.ac.jp.
Received June 22, 2016; Revised August 23, 2016; Editorial Decision December 18, 2016

ABSTRACT

Early stage oral cancer can be cured with oral brachytherapy, but whole-body radiation exposure status has not been previously studied. Recently, the International Commission on Radiological Protection Committee (ICRP) recommended the use of ICRP phantoms to estimate radiation exposure from external and internal radiation sources. In this study, we used a Monte Carlo simulation with ICRP phantoms to estimate whole-body exposure from oral brachytherapy. We used a Particle and Heavy Ion Transport code System (PHITS) to model oral brachytherapy with ^{192}Ir hairpins and ^{198}Au grains and to perform a Monte Carlo simulation on the ICRP adult reference computational phantoms. To confirm the simulations, we also computed local dose distributions from these small sources, and compared them with the results from Oncentra manual Low Dose Rate Treatment Planning (mLDR) software which is used in day-to-day clinical practice. We successfully obtained data on absorbed dose for each organ in males and females. Sex-averaged equivalent doses were 0.547 and 0.710 Sv with ^{192}Ir hairpins and ^{198}Au grains, respectively. Simulation with PHITS was reliable when compared with an alternative computational technique using mLDR software. We concluded that the absorbed dose for each organ and whole-body exposure from oral brachytherapy can be estimated with Monte Carlo simulation using PHITS on ICRP reference phantoms. Effective doses for patients with oral cancer were obtained.

KEYWORDS: brachytherapy, oral cancer, exposure, estimation, Monte Carlo simulation

INTRODUCTION

Early stage oral cancer can be effectively cured with oral brachytherapy, which can preserve patient quality of life [1, 2]. Our institution started offering this therapy in 1962. The high rate of control with this treatment has been achieved by inserting small radiation sources such as ^{192}Ir hairpins or ^{198}Au grains directly into lesions, which enables us to deliver high doses of radiation, up to 70 Gy per week, on a continuous basis [1]. However, there have been several reports that such interstitial radiotherapy inevitably causes whole-body exposure [3]. Matsubara *et al.* reported that in brachytherapy patients the equivalent whole-body dose is 0.5 Gy, based on the frequency of dicentrics and rings using data from the peripheral blood of actual patients [4]. There is a concern that such chromosomal changes might cause future radiation-induced malignancies [5, 6]. Thus, it would be important to ascertain whole-body radiation exposure status during oral brachytherapy treatment.

Physical models of the human body, such as the Rando phantom [7], with thermoluminescence dosimeters inside have been commonly used for evaluating radiation exposure. However, it would be difficult to actually insert radiation sources into the phantom. Recently, the International Commission on Radiological Protection Committee (ICRP) developed reference computational phantoms, which are based on medical imaging data from actual people and made compatible with data from previous ICRP publications. ICRP has recommended using these phantoms to estimate radiation exposure from internal and external radiation sources [8].

In this study, we used the ICRP Adult Reference Computational Phantoms and code for Monte Carlo simulation from the Particle and Heavy Ion Transport code System (PHITS) to estimate whole-body radiation exposure from oral cancer brachytherapy [9, 10].

METHODS

Treatment settings

In this study, we modeled two types of treatment that correspond to two kinds of small radiation sources under the assumption that they are being used to treat early-stage tongue cancer. Early stage tongue carcinoma corresponds to T1–2 N0 disease in the Union for International Cancer Control classification; the size of the largest local lesion is <4 cm. We usually select either ^{192}Ir hairpins or ^{198}Au grains (Fig. 1a and b, Chiyoda Technol Corp., Bunkyo-ku, Japan), depending on the thickness of the local lesion or patient performance status [2]. Typical placement of ^{192}Ir hairpins and ^{198}Au grains are shown in Fig. 1c and d, which can accommodate lesions with diameters up to 3 cm. ^{192}Ir hairpins are provided by the manufacturer three times per year; thus, the dose rate might differ depending on the time when the sources are implanted into patients. However, the prescribed dose for cancer control is ~70 Gy/5 days. This simulation was carried out using two 500 MBq ^{192}Ir hairpins for 120 h (equivalent to 24 h over 5 days; total of 4.2×10^8 disintegrations). ^{198}Au grains, which are used in permanent implants, are provided monthly. When used in patients, they are usually adjusted to 185 MBq each, and we aimed for a prescription dose of 80–90 Gy/∞, which corresponds to ~70 Gy over 7 days. The half-life of ^{198}Au grains is short, 2.695 days, and the cumulative dose was calculated to the decay of all sources. There were 6.2×10^8 MBq disintegrations.

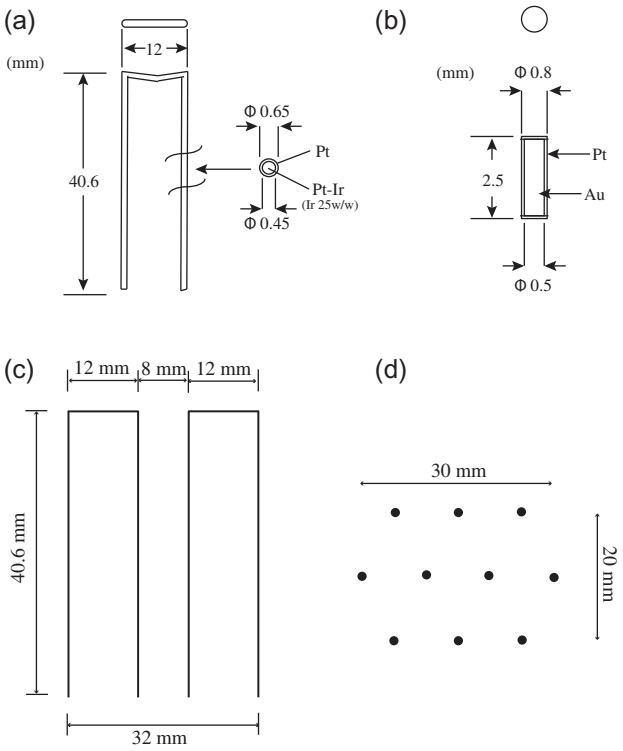

Fig 1. Schematic figure of (a) an ^{192}Ir hairpin and (b) a ^{198}Au grain and locations of (c) ^{192}Ir hairpins and (d) ^{198}Au grains during oral brachytherapy. (a) The figure shows an ^{192}Ir hairpin source, which has an inverted U-shape. Its diameter is 0.65 mm. It is made of a platinum and iridium alloy and coated with platinum. (b) The figure shows a ^{198}Au grain. It is a tiny source made of gold that is coated with platinum. (c) The figure shows the typical location of two ^{192}Ir hairpins, which could cover a tongue cancer lesion up to 32 mm long. For a larger lesion, an additional hairpin or a single pin would be placed 8 mm apart. (d) The figure shows the typical location of 10 ^{198}Au grains, which could cover a 30 × 20 mm oral cancer lesion. Grains should be placed 10 mm apart.

Monte Carlo simulation using PHITS

We employed PHITS version 2.52 as the Monte Carlo simulation code, running on the Windows 7 64-bit operating system [9]. PHITS has been used in simulations of therapeutic X-rays, particle radiation therapy, and Boron neutron capture therapy [10, 11]. In this study, we did not use the Electron Gamma Shower computation mode. The CPU was an Intel Core i5 unit (4 cores) with a clock speed of 2.80 GHz. The simulations were performed with the male and female ICRP adult reference computational phantoms [8]. The simulation computations were repeated 10^8 times per decay by PHITS. The cut-off energy in photons was set to 1 keV. The ICRP phantom is based on computed tomography voxel data, which are composed of 1.9 and 3.9 million voxels for the male and female phantoms, respectively. The dimension of each voxel was 2.1 × 2.1 × 8 mm^3 for a male who is 176 cm in height and 73 kg in weight, and 1.8 × 1.8 × 4.8 mm^3 for a female who is 163 cm in height and 60 kg in weight. Both phantoms contained 28 target organs. We made source models based on the schematic illustrations shown in Fig. 1a and b. For the ^{192}Ir hairpin source, we set the shape as shown in Fig. 1c, with a diameter of 0.45 mm. For the ^{198}Au grain source, the shape was set to 2.5 mm in length, with a diameter of 0.5 mm. The ^{192}Ir hairpins and ^{198}Au grains were located on the right border and dorsum of the tongue, respectively. The exact coordinates of the center of the ^{192}Ir hairpins in male and females were ($x = 2$, $y = -5.6$, $z = 70.97$ (cm)) and ($x = 2$, $y = -4.6$, $z = 65.97$ (cm)), respectively. Similarly, the coordinates of the ^{198}Au grains were ($x = 0$, $y = -5$, $z = 72.388$ (cm)) and ($x = 2$, $y = -5$, $z = 67.875$ (cm)), respectively. The photon radiation emitted was set according to the parameters shown in Table 1 [12]. ^{192}Ir undergoes electron capture and ß decay, and ^{198}Au only

Table 1. The emmission of photon energy and the release rate of ^{192}Ir and ^{198}Au

^{192}Ir		^{198}Au	
Photon energy (MeV)	Release ratio (%)	Photon energy (MeV)	Release ratio (%)
0.296	0.1385	0.078	0.02447
0.308	0.1448	0.412	0.96527
0.317	0.3991	0.676	0.00847
0.468	0.2307	1.088	0.00179
0.589	0.0217		
0.604	0.0396		
0.612	0.0256		

undergoes ß decay. Both radionuclides emit electrons; however, the electrons are stopped by the platinum-plating surface of each source [13]. Gamma rays and X-rays would be filtered out by the platinum plating, but its thickness is 0.1–0.15 mm and the reduced dose would be simulated to be <2%. Therefore, we considered the effect to be negligible and its simulation was omitted. Output data from PHITS consisted of the total heat quantity (MeV/cm^3) of each cell. The absorbed dose for each organ was obtained by converting the value in MeV/cm^3 units to J/kg (Gy), by multiplying it by 1.602×10^{-10} and dividing it by the determined organ mass provided by ICRP. In this study, the equivalent doses were equal to the absorbed doses, because the simulation was limited to only gamma rays and X-rays. The sex-averaged equivalent doses were obtained by averaging data from male and female absorbed doses. Finally, the effective dose from each radiation source was obtained as the sum of all the products of sex-averaged equivalent doses and corresponding tissue-weighting factors listed in Table 2, based on ICRP report 103 [14]. Totals for the tissue-weighting factors may not reach 1.000 because of rounding.

Confirmation of PHITS computations

To confirm whether the PHITS computation results were reliable, we performed an alternative computation using Oncentra Manual Low Dose Rate Treatment Planning software version 1.0 (mLDR) (Nucletron, Veenendaal, Netherlands) which is usually used in the hospital. Dose calculations are based on AAPM Task Group No. 43 Update 1 (AAPM-TG43U1) [15, 16]. The two types of small radiation sources were placed on an acrylic resin board as shown in Fig. 1, and two or three projection X-ray images were taken to virtually reconstruct the source locations in the software. The same settings for the radiation sources were used, and dose distribution lines were compared with the PHITS results. In addition, a representative point was selected for each dose distribution in the results from mLDR. The dose in the corresponding area (5 mm × 1 cm × 1 cm) was calculated with PHITS and compared with the absorbed dose for each radiation source.

Ethical declaration

Since no human or animal subjects were involved in this study, the ethical procedures were not applicable.

RESULTS

PHITS could successfully execute the programs, taking ~26 h for one series. The obtained data are shown in Table 2, in which male and female absorbed doses for each organ are listed in gray, and sex-averaged equivalent doses are given in sievert units. In most organs, absorbed doses were determined with relative statistical uncertainties of <1%. For organs distant from the head (e.g. colon, gonads, prostate/uterus, and urinary bladder wall), statistical uncertainties were as high as 10%. Effective doses for each source were calculated and shown on the bottom line in sievert. ^{192}Ir hairpins and ^{198}Au grains delivered effective doses of 0.547 Sv and 0.710 Sv, respectively. To confirm the computational reliability of PHITS, we also computed local dose distributions for both sources using PHITS (Fig. 2a and b) and compared them with the results from the mLDR software (Fig. 2c and d). In Fig. 2, the dose distributions are expressed in heat units [MeV/cm^3/source], which could be converted to Gy (J/kg), by multiplying them by 1.602×10^{-10} and the total number of disintegrations. In Fig. 2a, the dose distributions from the ^{192}Ir hairpins are shown, and the line for 10^{-3} heat [MeV/cm^3/source] corresponds to 68 Gy (calculated as $10^{-3} \times 1.602 \times 10^{-10} \times 4.2 \times 10^8$). This line is equivalent to the 70 Gy line in Fig. 2c. Similarly, a 10^{-3} dose distribution line from the ^{198}Au grains corresponds to 99 Gy (calculated as $10^{-3} \times 1.602 \times 10^{-10} \times 6.2 \times 10^8$), which is equivalent to the 90 Gy line in Fig. 2d. Representative points, A and B, were selected (Fig. 2c and d). The absorbed doses at these points were calculated using PHITS (Fig. 2e).

DISCUSSION

Although oral brachytherapy is associated with a high rate of local control in patients with oral cancer, it presumably results in some whole-body irradiation, based on studies of peripheral blood chromosomal aberrations [3, 4, 17]. This is a biological dosimetry counting method, which is believed to have high sensitivity and reliability. However, this method might be influenced by factors such as neoadjuvant chemotherapy, and it requires technical expertise for analysis. It is customary to use a Rando phantom to estimate radiation exposure from therapeutic and diagnostic radiation. However, this phantom is not suitable for estimating radiation exposure from transient internal radiation sources because this phantom is for an universal use, but it would be

Table 2. Each organ absorbed dose, sex-averaged equivalent doses, and effective doses from oral brachytherapy

Organ	Tissue weighting factor	^{192}Ir needle			^{198}Au grain		
		Absorbed dose (Gy)		Sex-averaged equivalent doses (mSv)	Absorbed dose (Gy)		Sex-averaged equivalent doses (mSv)
		male	female		male	female	
Bone marrow	0.12	0.287	0.423	355.04	0.278	0.432	354.75
Breast	0.12	0.103	0.255	179.02	0.082	0.202	141.64
Colon	0.12	0.014	0.009	11.71	0.010	0.006	7.88
Lungs	0.12	0.120	0.206	163.24	0.099	0.160	129.39
Stomach	0.12	0.039	0.043	41.14	0.029	0.035	31.99
Gonads	0.08	0.004	0.005	4.32	0.000	0.001	0.65
Liver	0.04	0.040	0.057	48.41	0.035	0.050	42.40
Oesophagus	0.04	0.398	0.716	556.77	0.305	0.506	405.46
Thyroid	0.04	0.704	1.510	1107.29	0.525	1.005	765.22
Urinary bladder wall	0.04	0.005	0.006	5.19	0.001	0.001	1.24
Endosteum	0.01	0.279	0.395	336.91	0.272	0.416	344.01
Brain	0.01	0.722	0.769	745.50	1.168	1.184	1175.86
Salivary	0.01	3.005	6.685	4845.01	2.269	4.007	3138.06
Skin	0.01	0.105	0.136	120.22	0.102	0.126	114.22
Adrenals	0.01	0.023	0.036	29.30	0.019	0.031	25.36
Extrathoracic region	0.01	4.208	6.903	5555.67	8.571	9.738	9154.32
Gall bladder wall	0.01	0.030	0.041	35.14	0.024	0.038	31.03
Heart	0.01	0.102	0.180	140.77	0.080	0.137	108.10
Kidneys	0.01	0.016	0.024	20.20	0.013	0.020	16.79
Lymphatic nodes	0.01	0.151	0.211	180.82	0.118	0.170	143.68
Muscle	0.01	0.171	0.172	171.40	0.178	0.153	165.56
Oral mucosa	0.01	29.584	27.942	28763.05	39.616	56.025	47820.11
Pancreas	0.01	0.024	0.029	26.70	0.019	0.024	21.52
Prostate/Uterus	0.01	0.004	0.004	4.15	0.000	0.002	1.02
Small intestine	0.01	0.011	0.013	12.21	0.007	0.009	8.21
Spleen	0.01	0.037	0.052	44.56	0.029	0.039	33.63
Thymus	0.01	0.331	0.591	461.21	0.249	0.419	333.69
Lenses of eye	-	1.542	1.586	1563.80	2.362	2.763	2562.18
Effective dose (mSv)				546.73			710.35

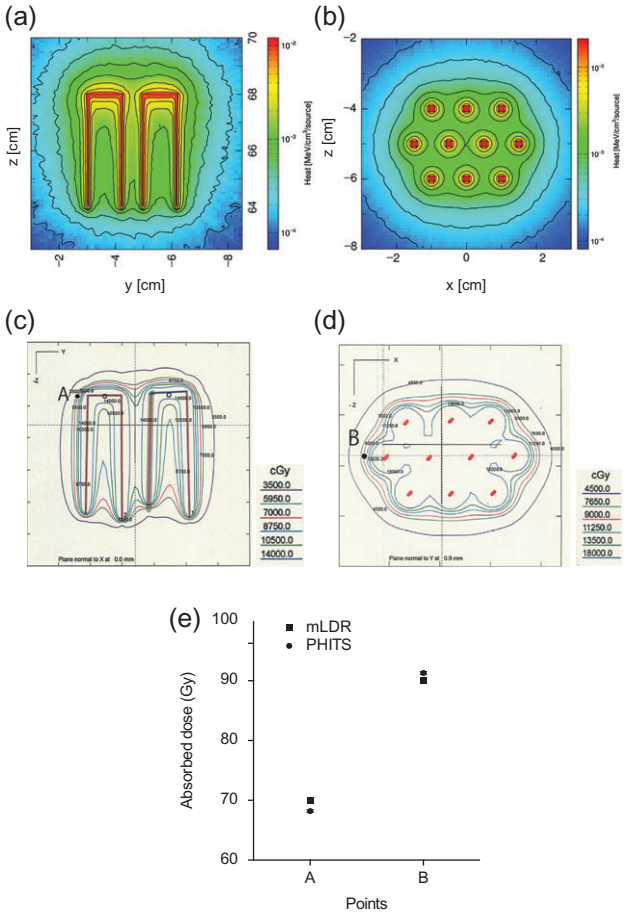

Fig 2. Comparison of the local dose distributions computed by the PHITS simulation code (a) and (b) and mLDR clinical software (c) and (e). The 10^{-3} line for the ^{192}Ir hairpins (a; overview) corresponds to the 70 Gy line (red) (c), and the 10^{-3} line for the ^{198}Au grains (b) corresponds to the 90 Gy line (d). The results from PHITS (a and b) could be compared with those from mLDR (c and d). Dose distributions for ^{192}Ir hairpins and ^{198}Au grains from PHITS were similar to those from mLDR. Point A in (c) and Point B in (d) were selected as representative 70 Gy and 90 Gy dose points, respectively. The dose was also calculated with PHITS (e). The data from PHITS are represented as mean values with statistical error bars. Error bars are not shown for mLDR data because they dose not calculate them. There were slight differences between mLDR and PHITS results, but the difference was ~2.6% for ^{192}Ir hairpins and ~1.4% for ^{198}Au grains.

impossible to be milled if the real sources would be implanted in it. In addition, it would be difficult to purchase small sources for the purpose of such a study. Nowadays, we can perform Monte Carlo simulation on ordinary personal computers with ICRP computational phantoms.

In this study, we used PHITS for Monte Carlo simulation code. We computed the local dose distributions and doses for each organ using small source models. We evaluated the computational reliability of PHITS by comparing the results with those from mLDR, which is based on AAPM-TG43U1 [15, 16]. TG43U1 offers an easy method for computing the dose distribution, but it requires a situation in which radiation equilibrium scatter conditions, and is weak to interseed attenuation [18]. Therefore, it cannot be used for estimating whole-body exposure. On the other hand, Monte Carlo simulation using PHITS can be used for local or whole-body exposure, but it is computationally intensive. We were not certain whether it was executed as designed. Therefore, we compared the results from PHITS with those from mLDR. The dose distributions from PHITS and mLDR were similar, but dose comparisons at representative points showed that there were slight differences (Fig. 2e). However, the difference was ~2.6% for ^{192}Ir hairpins and ~1.4% for ^{198}Au grains, indicating that the results for each organ in the whole-body model would be accurate in the range of several percentage differences.

As a result, we could successfully obtain absorption dose values for each organ in the male and female phantoms, as well as sex-averaged equivalent dose values, as shown in Table 2. In general, the absorbed doses in each organ were higher in females, possibly due to smaller body size. Turning our attention to the radiation sources, the values for areas such as oral mucosa, extrathoracic region, lens of the eye, and brain were higher for ^{198}Au grains than for ^{192}Ir hairpins. For the other organs, absorbed doses were higher for ^{192}Ir hairpins than for ^{198}Au grains, despite sex differences, mainly because the source locations for ^{198}Au grains are more compact and slightly more cranially located than the locations for ^{192}Ir hairpins, but the ^{192}Ir hairpins were longer (4.06 cm) in the cephalocaudal axis, as shown in Fig. 1.

The effective dose of the ^{192}Ir hairpins and ^{198}Au grains were 0.547 and 0.710 Sv, respectively, which are equivalent to the results for 0.5 Gy obtained by Matsubara *et al.* [4]. These doses may depress hematological function [19]. Matsubara *et al.* reported that the peripheral lymphocyte count of their patients temporarily decreased by 50% or more, but no bone marrow death was observed. As for other deterministic effects, the absorbed dose for the lens of the eye reached the threshold dose of 0.5–2.0 Gy [20], which is associated with a 1% incidence of lens opacity, but at this dose it is unlikely to progress to cataracts. We have not previously taken a clinical interest in this possibility, but for recurrent cases, we sometimes repeat this treatment two or three times [21]. In this scenario, the cumulative dose could possibly reach the threshold value of 5 Gy for cataracts, and it is necessary for us to inform patients of this possibility in advance. Oral mucosa was exposed to doses of 28–56 Gy, which always causes acute mucositis after brachytherapy. However, this therapy is not associated with other deterministic effects such as infecundity or teratogeny. Stochastic effects from exposure are also of concern. In brachytherapy, photon radiation from small sources is used to treat cancer. It rarely induces another neoplasm in the future. The ICRP committee indicated a risk coefficient of 0.055 events per Sv on the basis of cancer risk [14], resulting in a 0.3% or 0.39% risk of cancer-related death. We previously published data about radiation-induced cancers, and concluded that the crude incidence of them is 1.4–1.8%, which corresponds to a handful of cases [6]. Hence, it would be difficult to work out a reliable number of cancer-related deaths from our

experience only. Concerning hereditary risk, most oral cancers occur in persons in their sixties in Japan, and hereditary effects might be of little consequence, but we can calculate it by multiplying the effective doses by 0.002, which results in 0.001% [14]. However, these values for cancer risk and hereditary risk might be acceptable, because patients could obtain a higher quality of life from oral brachytherapy for treatment of oral cancer [2]. In this study, we estimated the absorbed dose for each organ and whole-body exposure from brachytherapy in patients with oral cancer. The estimated effective dose was 0.547 Sv from ^{192}Ir hairpins and 0.710 Sv from ^{198}Au grains. We can apply this knowledge to clinical situation.

CONFLICT OF INTEREST

All authors declare that they have no conflicts of interest.

FUNDING

This study was supported by the Grants from Ministry of Education, Culture, Sports, Science and Technology-Japan, called as MEXT. The Grants number is MEXT 16K11498. It would be enough information following the Japanese Government instructions.

REFERENCES

1. Oota S, Shibuya H, Yoshimura R et al. Radiotherapy of stage II mobile tongue carcinoma. Prediction of local control and QOL. *Radiat Oncol* 2006;1:21.
2. Yoshimura R, Shibuya H, Miura M et al. Quality of life of oral cancer patients after low-dose-rate brachytherapy. *Int J Radiat Oncol Biol Phys* 2009;73:772–8.
3. Boyd E, Feruguson-Smith MA, MacDougall IR et al. Chromosome breakage in human peripheral lymphocytes after radioactive iodine (^{125}I) treatment. *Radiat Res* 1974;57:482–7.
4. Matsubara S, Horiuchi J, Okuyama T et al. Chromosome aberrations in the peripheral lymphocytes induced by brachytherapy and external cobalt telegraphy. *Int J Radiat Oncol Biol Phys* 1985;11:1085–94.
5. Hall EJ. *Radiobiology for the Radiologist.* 5th ed. Philadelphia: Lippincott Williams and Wilkins, 2000.
6. Amemiya K, Shibuya H, Yoshimura R et al. The risk of radiation-induced cancer in patients with squamous cell carcinoma of the head and neck and its results of treatment. *Br J Radiol* 2005;78:1028–33.
7. Alderson SW, Lanzl LH, Rollins M et al. An instrumented phantom system for analog computation of treatment plans. *Am J Rontgenol* 1962;87:185–95.
8. ICRP. *Adult reference computational phantoms*. ICRP Publication 110. *Ann ICRP* 2009;39 (2).
9. Sato T, Niita K, Matsuda N et al. Particle and heavy ion transport code system, PHITS, version 2.52. *J Nucl Sci Technol* 2013; 50:913–23.
10. Ohno Y, Torikoshi M, Suzuki M et al. Dose distribution of a 125kV mean energy microplanar x-ray beam for basic studies on microbeam radiotherapy. *Med Phys* 2008;35:3252–8.
11. Baba H, Onizuka Y, Nakao M et al. Microdosimetric evaluation of the neutron field for BNCT at Kyoto University reactor by using the PHITS code. *Radiat Prot Dosim* 2011; 143:528–32.
12. Japan RadioIsotope Association. *Radioisotopes Pocket Data Book*. Tokyo: Maruzen Co. Ltd, 2003.
13. Japan Radioisotope Association. *Isotope Handbook*. 3rd edn. Tokyo: Maruzen Co. Ltd, 1995.
14. ICRP Publ.103: *Recommendations of the ICRP*, Exeter, UK: ICRP; 2007.
15. Rivard MH, Coursey BM, DeWerd LA et al. Update of AAPM Task Group No. 43 report. A revised AAPM protocol for brachytherapy dose calculations. *Med Phys* 2004;31:633–74.
16. Van der Laarse R, Granero D, Perez-Calatayud J et al. Dosimetric characterization of Ir-192 LDR elongated sources. *Med Phys* 2009:35:1154–61.
17. Lloyd DC, Purrott RJ, Dolphin GW et al. A comparison of physical and cytogenetic estimates of radiation dose in patients treated with iodine-131 for thyroid carcinoma. *Int J Radiat Biol* 1976;30:473–85.
18. Tanaka K, Kamo K, Tateoka K et al. A comparison of the dose distributions between the brachytherapy ^{125}I models, STM1251 and Oncoseed 6711, in a geometry lacking radiation equilibrium conditions. *J Radiat Res* 2015;56:366–71.
19. ICRP. *Nonstochastic effects of ionizing radiation*. ICRP Publication 41. *Ann ICRP* 1984;14(3).
20. Otake M, Schull WJ. Radiation-related posterior lenticular opacities in Hiroshima and Nagasaki atomic bomb survivors based on the DS86 dosimetry system. *Radiat Res* 1990;12:3–13.
21. Ayukawa F, Shibuya H, Yoshimura R et al. Curative brachytherapy for recurrent/residual tongue cancer. *Strahlenther Onkol* 2007;183:133–7.